The Role of Flight Tests and Wind Tunnels in Laminar Flow Research

Horst Körner and **Günter Redeker**
Deutsche Forschungsanstalt für Luft- und Raumfahrt e.V. (DLR)
Institute of Design Aerodynamics
Postfach 3267, D-38022 Braunschweig

Abstract

Laminarization of wetted surfaces on subsonic/transonic transport aircraft is one of the big challenges of the next decade. Physical phenomena have to be clarified and design tools to be developped. The new technology must be validated in order to be applied in new aircraft.

More than in current technologies flight tests play a major role in the development of this new technology. This is due to the fact that the transition laminar/turbulent is dominantly influenced by the flow turbulence and/or noise which have different levels in flight and in wind tunnels. Furthermore surface imperfections and contamination are critical features for the maintenance of laminar flow which also require flight tests.

This paper will review flight testing for laminar flow research and will briefly describe the situation of the wind tunnels in this field.

1. Introduction

Laminar flow technology offers a large potential in drag reduction for subsonic transport aircraft [1-4]. Originally used and developped for sailplanes and smaller aircraft this technology is now under serious consideration for large transport aircraft. In a mid term drag reductions of 15 % to 20 % may be achieved for this type of aircraft, in a long term and accompanied by other advanced technologies 50 % drag reduction is the prospect. Thus, laminarization of aircraft surfaces promises a remarkable amount of fuel saving resulting in a higher efficiency of the aircraft combined with a reduction of the environmental pollution. Major research programs to mature the laminar flow technology are executed in the USA and in Europe [5,6].

There are in principle different techniques to realize laminar flow:

- Natural laminar flow (NLF)
- Laminar flow control (LFC)

and a combination of both

- Hybrid laminar flow control (HLFC).

NLF takes advantage from the fact that the stability of the laminar boundary depends on the pressure gradient and the Reynolds number [7]. Thus, for twodimensional boundary layers laminar flow can be maintained by adjusting the pressure gradient according to the Reynolds number. At high Reynolds numbers and swept wings NLF is not sufficient to generate laminar boundary layers. Thus, surface suction has to be added to get laminar flow (LFC).

Especially for transonic transport aircraft a proper combination between NLF and LFC may lead to HLFC, where suction is only applied in the leading edge region to control the crossflow instability.

Laminarization is a technique which has already been known since more than fifty years but has not been applied until now except for sailplanes and smaller aircraft. The reason for this was that some basic prerequisites have to be fulfilled which were outside the scope in the past.

Firstly, a deeper insight in the transition mechanisms of threedimensional laminar boundary layers on swept wings and a reliable transition prediction procedure have to be available. As outlined later this has been achieved by means of linear stability analysis. Secondly, CFD-methods for calculating basic flows around airfoils and wings including viscous effects can be used with great confidence. Thirdly, a good surface quality with regard to roughness, waviness and manufacturing excrescences is nowadays feasible by means of new manufacturing techniques of composite structures. Furthermore, surfaces for suction systems can be manufactured by using laser- or electronic-beam drilled holes with small diameters. Fourthly, solutions for protecting wing surfaces against contamination by insect debris which destroy the laminar boundary layer are under development.

Classical tool for the aerodynamic development of aircraft is the wind tunnel. Due to wind tunnel turbulence and noise, transition is different in wind tunnel compared to free flight. Therefore, the use of wind tunnels in the development of laminar flow aircraft has to be considered under new aspects and a good correlation of the wind tunnel results with free flight results should be possible. Thus, flight testing in laminar flow research is irrevocable.

This paper will give a survey of the role of both tools with special attention to the transition process laminar/turbulent. Chapter 2 gives a short description of the theoretical background of the transition mechanisms and the related transition prediction procedures. Chapter 3 gives an overview over typical flight tests for laminar flow research, while chapter 4 elucidates the role of wind tunnels in this field.

Copyright © 1994 by ICAS and AIAA. All rights reserved.

2. Transition and transition prediction in threedimensional boundary layers

On swept wings threedimensional laminar boundary layers occur with skewed velocity profiles. The transition process in such boundary layers can be described by the following mechanisms or combination of these (**Fig. 2.1**) [8]:

- Transition due to Tollmien-Schlichting-instability (TSI) known from the twodimensional case which on a swept wing normally occurs in the middle part of the wing.
- Transition due to crossflow-instability (CFI) which is caused by strong cross pressure gradients and which normally takes place near the leading edge.
- Attachment line transition (ALT) which occurs at the attachment line of swept wings.

For the design of laminar flow swept wings reliable transition prediction procedures for these types of transition mechanisms should be available. Neither the empirical correlations for the twodimensional type of transition [9,10], nor the procedure established in [11] for the crossflow type of transition seem to work satisfactory for high Reynolds numbers.

Thus, the main objective is to develop a transition prediction procedure for engineering purposes with the aid of the linear stability theory of laminar boundary layers. The main principles have been already described [12] and the application has been demonstrated in [8,13]. Based on experimental results - measured pressure distributions and transition locations - stability calculations by linear stability theory provide limiting N-values or N-factors at the measured transition location. It is assumed that each transition mechanism corresponds to a limiting N-value. Thus, in the application of the stability analysis only disturbance modes are taken into account which are characteristic for the respective instability. Therefore the following integration strategy for N-factors [14] have been used:

The N-factor due to TSI N_{TS} is calculated in the fixed frequency mode with high frequency disturbances propagating in the direction of the mean flow ($\psi = 0°$). The N-factor due to CFI N_{CF} is calculated in the fixed wave length mode for zero frequency disturbances propagating in the cross flow direction. That means only steady crossflow vortices are considered and higher frequency disturbances are not taken into account. It is further assumed that no interaction between CFI and TSI will take place.

This assumption can be confirmed by a stability analysis of swept wing wind tunnel results (**Fig. 2.2**) after [15] calculated as described above with the SALLY-code [16]. It turns out that crossflow amplification starts immediately after the leading edge and reaches high N-values whereas Tollmien-Schlichting-amplification starts more downstream at 10 % of the wing chord with a relatively low increase. The so obtained results will be correlated by experimentally determined transition locations so that limiting N-values N_{TS} and N_{CF} can be determined.

For unswept wings (2D boundary layer) one limiting N-value the N_{TS}- value can be specified. For swept wings the two limiting N-values can be plotted in an N_{TS}-N_{CF} diagramme as shown in **Fig. 2.3**. The region below the curve indicates laminar boundary layers and above turbulent ones. Three different types of curves may be expected. The concave type of curve represents the case of a strong interaction between TS- and CF-instability which leads to a remarkable reduction in amplification factors. The straight line represents the case of a moderate interaction indicating that $N_{CF} + N_{TS} = \text{const.}$ The more convex type of the curve will show that only a weak interaction between CFI and TSI will take place.

It can be stated that the magnitude of the limiting N-values depends on the quality of the flow. It turns out that the highest limiting N-values are achieved in flight tests, where the flow is nearly free of turbulence and disturbances. Lower values are assumed to occur in wind tunnel flows where wind tunnel turbulence and noise degrade the flow quality. Thus, the limiting N-values of a wind tunnel are specific figures for that wind tunnel and characterize the transition behaviour. They differ from wind tunnel to wind tunnel and are generally lower than those obtained in free flight.

Thus, well-designed laminar flow experiments can only be carried out if the limiting N-values are known in advance. Keeping this in mind different types of laminar flow experiments can be identified:

- Experiments clarifying the physical phenomena of transition,
- experiments in wind tunnels and flight establishing limiting N-values,
- experiments for varifying aerodynamic designs and performance testing and
- experiments for clarifying operational aspects of laminar flow.

Some of these experiments in flight and in wind tunnels are briefly discussed in chapter 3 and chapter 4 of this paper.

3. Flight test for laminar flow research

This chapter provides a survey on flight tests carried out at the Institute of Design Aerodynamics or with its participation.

First flight tests to validate natural laminar flow airfoils for gliders have been carried out on the flying test-bed based on the research sailplane "Janus" [17]. A series of airfoils have been tested in the Reynolds number range of $Re \approx 3 \cdot 10^6$ under realistic flight conditions.

For higher Reynolds numbers on unswept and swept wings flight tests have been carried out to develop an engineering transition prediction procedure based on linear stability analysis of laminar boundary layers, the so-called N-factor method, briefly described in chapter 2.

For unswept wings and Reynolds numbers up to $Re \approx 10 \cdot 10^6$ the research aircraft LFU-205 of DLR was used (**Fig. 3.1**). This propeller driven aircraft was equipped with a partly modified wing surface (glove) [18] suitable for an N-factor determination in flight. Pressure distributions have been measured and transition locations have been determined by means of infrared image technique at various flight conditions by changing flight height and flap deflection of the wing.

From these tests limiting N_{TS}-values at the experimentally determined transition locations have been calculated with the linear stability theory using the measured pressure distributions. A nearly constant limiting N-value of $N_{TS} \approx 13.5$ was the outcome of these flight tests [18] which was independent of the flight conditions. Results will be shown later in chapter 4 together with wind tunnel tests. The so obtained N_{TS}-value will be used later in the design process of laminar flow unswept wings.

In order to verify that the linear stability analysis of laminar boundary layers is a useful and reliable tool in transition prediction details of the transitional laminar boundary layer have been measured in flight with the same aircraft. A hot-wire traversing device has been mounted inside the wing which could be operated computer controlled and which was able to measure boundary layer velocity profiles as well as velocity fluctuations [19]. At different chordwise positions boundary layer traverses have been measured and compared with linear stability theory results.

Fig. 3.2 shows a frequency spectrum of measured disturbances at a chordwise position of 43 % of the wing. This is in front of the transition location which took place at 55 % at this test point. In the region of 900 Hz to 1200 Hz an amplification of disturbances can be noticed in the measured spectrum. This compares well with amplified Tollmien-Schlichting waves calculated at this station by means of linear stability theory, where N_{TS}-values of $N_{TS} \approx 10$ are already achieved. Furthermore, a good comparison of measured and calculated wave-lengths of TS-waves have been found. Thus, these tests revealed that linear stability theory is able to predict the main features (frequencies and wave-lengths) of a transitional boundary layer with a high confidence, although nonlinear effects which governs transition are not covered. LFU-205 will be used in the near future to investigate the propagation of wave packages.

For swept wing aircraft and higher Reynolds- and Mach-number the DLR-research aircraft VFW 614/ATTAS (**Fig. 3.3**) has been used to determine the limiting N-values. These investigations have been carried out in close cooperation with Deutsche Aerospace Airbus. The VFW 614/ATTAS aircraft has been equipped with a laminar flow glove designed for the special purpose of N-factor determination [20]. The design was done in such a way that a large flexibility in generating transition by different mechanisms could be achieved. By changing flight height, angle of yaw and flap deflections transition could be changed from the Tollmien-Schlichting-instability type to the crossflow type. The measurement techniques used were the same as in the LFU-205 flight tests [21]. Pressure measurements and infrared inspection of the glove surface provide sufficient information to carry out the stability analysis.

Fig. 3.4 shows a typical example of transition location behaviour by changing angle of yaw from $\beta = 3^\circ$ to $\beta = -3^\circ$. At $\beta = 3^\circ$ and 0° yaw angle the transition lines coincide and transition occurred due to Tollmien-Schlichting-instability. At $\beta = -3^\circ$ (increased sweep angle) the transition line moved rapidly upstream and became saw-toothed. This behaviour could be observed at all data points where transition occurred due to crossflow-instability.

The stability analysis of many flight test points is shown in **Fig. 3.5**. The measured glove pressure distributions are evaluated by means of the incompressible SALLY-code [16] as explained in chapter 2. The data points in Fig. 3.5 indicates as already discussed in chapter 2 that there is only a weak interaction between Tollmien-Schlichting waves and crossflow-vortices for the investigated laminar flow glove on VFW 614/ATTAS.

Thus, with Fig. 3.5 and the limiting N_{TS}-value of $N_{TS} = 13.5$ for unswept wings more sophisticated and reliable transition prediction criteria for unswept and swept wings have been established in flight, which could be used in the design process of laminar flow wings.

In a first example the gained experiences have been used to prepare flight tests on the DLR-research aircraft Dornier Do 228 together with the Dornier GmbH. The main objectives of these flight tests for a commuter type aircraft were to investigate

- the performance of a laminar flow wing in flight,
- manufacturing excrescences, as steps, gaps and joints, rivet heads a.s.o.,
- the influence of the propeller slipstream on a laminar flow wing and
- a contamination avoidance system.

For this purpose the Do 228 was equipped with a laminar flow wing glove outside of the engine nacelle. **Fig. 3.6** shows the airplane equipped with the laminar flow glove and the measuring equipment. It is interesting to notice that a movable wake rake has been established behind the wing glove to measure wing section drag in flight. The flight tests revealed that the laminar flow glove design fulfilled all the requirements and very low drag coefficients of $c_D \approx 0.0038$ have been measured as shown in **Fig. 3.7**. More details of these flight tests will be reported in [22] on the occasion of the congress. From the viewpoint of this paper it is interesting to note that the outlined transition prediction procedure worked excellent in the preparation of these tests.

The second example is the design of a laminar wing full chord glove for the Fokker F 100 aircraft (**Fig. 3.8**) with a swept wing of 20° leading edge sweep. These investigations have been carried out within the BRITE/EURAM programme initiated by the European Community in the research project ELFIN [23] together with several European partners from industry and research. The objectives of these tests was also the proof of the aerodynamic performance of a laminar flow wing glove in flight. The results obtained so far fully confirmed the design objectives and laminar boundary layers up to 50 % of wing chord have been achieved.

Another flight experiment on the VFW 614/ATTAS is related to engine-nacelle flow (**Fig. 3.9**). In cooperation with Rolls-Royce and MTU a natural laminar flow nacelle has been designed, built by Hurel/Dubois and flight tested [24]. As in the wing glove cases the design was accomplished by using CFD-methods for the basic flow and the N-factor method for transition prediction. The flight tests revealed that laminar flow over 60 % of the nacelle chord was achieved. In a second test campaign a nacelle segment equipped with a suction system and a contamination avoidance system has been tested. The evaluation of these results is still in progress.

Flight tests with regard to operational aspects are discussed in details in [22] on the laminar flow glove of the Dornier Do 228, where a liquid contamination avoidance system and manufacturing excrescences have been investigated.

4. Wind tunnel tests for laminar flow research

It is obvious that not all laminar flow research investigations can be done in free flight experiments with its ideal disturbance free environment. There are mainly two reasons for this: Flight experiments are generally very costly and in the case of an aircraft development a demonstrator aircraft for flight tests is not available in advance. Therefore, wind tunnels have to be used in laminar flow testing.

A reasonable operation of wind tunnels is possible if the flow has been calibrated with respect to the transition behaviour of laminar boundary layers; that means a determination of the limiting N-values N_{TS} and N_{CF} has been carried out. Examples for such a calibration for various wind tunnels are shown in the next figures. **Fig. 4.1** shows the N_{TS}-value obtained in the 6m x 8m test section of the Dutch-German-Wind-Tunnel (DNW) with the wing of the LFU-205 [18]. Values of $N_{TS} = 13.5$ have been achieved in the wind tunnel which is nearly the same value of the free flight experiments. This demonstrates the excellent flow quality of DNW for laminar flow testing.

Fig. 4.2 shows N_{TS}-values for different wind tunnels (subsonic and transonic ones). The values vary between 14 (T2 transonic wind tunnel of ONERA [25], DNW as mentioned above) and 5 (TWB transonic wind tunnel of blow down type of DLR [26]). Although the N_{TS}-values of the TWB-wind tunnel seems to be very low it has been proven that reasonable laminar flow experiments can be carried out in such a wind tunnel.

Fig. 4.3 demonstrates the limiting N_{TS}- and N_{CF}-values of the ONERA-S1MA wind tunnel in comparison with flight experiments [27]. It is shown that not only the N_{CF}-values have decreased but also the N_{TS}-values of the wind tunnel are smaller than those obtained in flight experiments.

Limiting N-values allow a better assessment of the use of a wind tunnel in laminar flow testing than the conventional turbulence level [25]. This is due to the fact that the N-factors do not consider all disturbance frequencies with the same weighting function but only those frequencies which are decisive for the transition process.

This is demonstrated schematically in **Fig. 4.4**. In the upper part of the figure a frequency spectrum of a wind tunnel with large disturbances in the low frequency range is shown. If a laminar boundary layer is considered with amplification of disturbances - e.g. TS-waves - in the moderate frequency range, less influence of the wind tunnel disturbances on the transition behaviour is expected. In the lower part of the figure the frequency disturbance spectrum of the wind tunnel is in the same range as the boundary layer disturbance frequencies. Thus, a resonance between wind tunnel disturbances and boundary layer TS-waves will occur and will influence the transition behaviour strongly.

Although laminar boundary layers are influenced in an adverse manner by the wind tunnel flow that means premature transition occurs compared to free flight condition due to lower N-values, wind tunnels are still useful in carrying out these tests.

The next figures will give an example for a transonic transport aircraft with a laminar flow wing to be tested in a wind tunnel [25].

Fig. 4.5 presents the stability relations of a wing section of a full scale aircraft in a N_{TS}-N_{CF}-diagramme. This graph presents the limiting N-values for free-flight conditions and the variation of N-factors along the wing chord of a wing section for the full scale configuration. In the front part of the wing crossflow instability is strongly amplified (large N_{CF}-values) whereas the Tollmien-Schlichting-waves are damped ($N_{TS} \approx 0$). From 20 % of wing chord on the N_{TS}-value grows due to amplified TS-waves whereas the N_{CF}-values remain relatively constant due to small cross pressure gradients in that region. At $x/c \approx 0.5$ N_{TS}– and N_{CF}–values exceed the limiting curve indicating that transition from laminar to turbulent flow have taken place at that chordwise station.

Fig. 4.6 describes the same situation in a wind tunnel. The curves for the full-scale conditions are marked here by dotted lines. The curve of limiting N-values for the wind tunnel indicates decreasing limiting N-values for N_{TS} as well as for N_{CF}. If in the wind tunnel tests the same Reynolds number can be achieved as in free flight transition due to crossflow-instability at the leading edge is visible. Thus, the wind tunnel test will lead to wrong conclusions. On the other hand if wind tunnel tests at a reduced Reynolds number are carried out the same stability behaviour of the wing section in the wind tunnel can be achieved as in free flight as shown by the full line. Thus, transition in the wind tunnel also takes place at 50 % of the wind chord.

These example may show that the wind tunnel also is a reasonable tool for laminar flow experiments if these experiments are analysed by stability analysis and if the limiting N-values of the wind tunnel are known.

5. Conclusions

The laminar flow technology is one of the key technologies for aircraft of the next century. It promises a large potential in drag reduction connected with a remarkable amount of fuel savings and a reduction in pollution of the environment. Therefore, this technology is subject of research worldwide.

As CFD today is not able to offer practical solutions for realistic configurations research mainly is relying on experimental investigations in flight and/or in wind tunnels. This paper points out to what extent flight testing is necessary to mature the laminar flow technology and how existing wind tunnels can be used to participate in the research work. It turns out that wind tunnel investigations besides flight tests can provide reasonable results provided that a suitable calibration of the wind tunnel flow with regard to free flight behaviour of laminar flows by means of stability analysis of laminar boundary layers have been carried out. Example of such a calibration and the application to wind tunnels are briefly discussed.

References

[1] W. Pfenninger
Laminar Flow Control, Laminarization.
AGARD-R-654 (1977), pp. 3-1 to 3-75.

[2] R. Hilbig, H. Körner
Aerodynamische Entwicklungsrichtungen für Verkehrsflugzeuge.
DGLR-Jahrbuch 1984, Bd. I, S. 82-1 bis 52 (1986).

[3] H. Körner, K.H. Horstmann, H. Köster, A. Quast, G. Redeker
Laminarization of Transport Aircraft Wings - A German View.
AIAA-Paper-87-0085 (1987).

[4] H. Körner
Natural laminar flow research for subsonic transport aircraft in the FRG.
Z. Flugwiss. Weltraumforsch. 14 (1990), pp. 223-232.

[5] R.W. Barnwell, M.Y. Hussaini (Eds.)
Natural Laminar Flow and Laminar Flow Control.
ICASE/NASA LARC Series.
Springer, New York, Heidelberg, London, 1992.

[6] -
Proceedings of the "First European Forum on Laminar Flow Technology".
DGLR-Bericht 92-04, 1992.

[7] H. Schlichting
Boundary-Layer Theory.
7. Ed., McGraw-Hill, New York, 1979.

[8] G. Redeker, K.H. Horstmann, H. Köster, A. Quast
Investigations on high Reynolds number laminar flow airfoils.
Journ. Aircraft, Vol. 25, (1988) pp. 583-590.

[9] P.S. Granville
The calculation of the viscous drag of bodies of revolution.
David Taylor Model Basin Rep. 849, 1953.

[10] R. Michel
Critère de transition et amplification des ondes d'instabilité laminaire.
La Recherche Aérosp. No. 70, 1959.

[11] D. Arnal, M. Habiballah, E. Coustols
Laminar instability theory and transition criteria in two- and threedimensional flow.
Rech. Aerosp. 1984-2, 1984, pp. 45-63.

[12] J. Runyan, D. George-Falvy
Amplification factors at transition on an unswept wing in free flight and on a swept wing in wind tunnel.
AIAA paper No. 70-0267, 1979.

[13] G. Redeker, K.H. Horstmann
Die Stabilitätsanalyse als Hilfsmittel beim Entwurf von Laminarprofilen.
DGLR-Ber. 86-03, 1986, pp. 317-348.

[14] H. Bieler, G. Redeker
Entwicklung von Transitionskriterien auf e^N-Basis für dreidimensionale Flügelgrenzschichten.
DGLR-Ber. 88-05, 1988, pp. 103-116.

[15] F.W. Boltz, G.C. Kenyon, C.Q. Allen
Effects of sweep angle on the boundary layer stability characteristics of an untapered wing at low speeds.
NASA TN-D 338, 1960.

[16] A.J. Skrokowski, S.A. Orszag
SALLY level II user's guide. COSMIC Program No. LAR-12556, 1979.

[17] H. Körner, K.H. Horstmann
The use of airplanes for aerodynamic research at DFVLR - Institute of Design Aerodynamics.
Festschrift for B.H. Goethert's 80th Birthday, University of Tennessee, Tullahoma, 1987.

[18] K.H. Horstmann, A. Quast, G. Redeker
Flight and Wind Tunnel Investigations on Boundary Layer Transition.
J. Aircraft, Vol. 27, pp. 146-150 (1990).

[19] K.H. Horstmann, S.J. Miley
Comparison of Flight and Wind Tunnel Investigations of Tollmien-Schlichting Waves on an Aircraft Wing.
In [6], pp. 45-51 (1992).

[20] G. Redeker, K.H. Horstmann, H. Köster, P. Thiede, J. Szodruch
Design of a Natural Laminar Flow Glove for a Transport Aircraft.
AIAA Paper 90-3043, 1990.

[21] K.H. Horstmann, G. Redeker, A. Quast, U. Dressler, H. Bieler
Flight Tests with a National Laminar Flow Glove on a Transport Aircraft.
AIAA Paper 90-3044, 1990.

[22] W. Wohlrath, H. Echtle, P. Dick, D. Welte, H.-W. Stock, B.Moeken, K.H. Horstmann, R Müller, C.H. Rohardt, A. Quast
Design and Flight Test Evaluation of a Laminar Wing Glove on a Commuter Aircraft.
ICAS Conference Proceedings; 19th. ICAS Congress, Anaheim, Ca., Paper No. ICAS-94-5.4.1 (1994).

[23] H. Dziomba, A. Davies, H. Stock, N. Voogt
ELFIN-European Laminar Flow Investigations.
Conference Proceedings, Aeronautics Days 1991, Brussels, pp. 37-50.

[24 B. Barry, S. Parke, N. Brown, H. Riedel, M. Sitzmann
The Flight Testing of National and Hybrid Laminar Flow Nacelles.
39th IGI Congress (ASME), June 1994.

[25] G. Redeker
Die zukünftige Rolle der Windkanäle bei der Entwicklung von Laminarflügelflugzeugen.
DGLR-Jahrbuch 1993, Vol. III, (1993), Beitrag 93-03-019.

[26] H. Köster, R. Müller
Bestimmung des N-Faktors im Transsonischen Windkanal Braunschweig (TWB) anhand von Druckverteilungs- und Umschlagpunktmessungen und dem SALLY-Verfahren.
DGLR-Bericht 88-05, (1988) pp. 77-92.

[27] R. Henke, F.X. Münch, A. Quast
Natural Laminar Flow: A Wind Tunnel Test Campaign and Comparison with Flight Test Data.
AIAA Paper 90-3045, 1990.

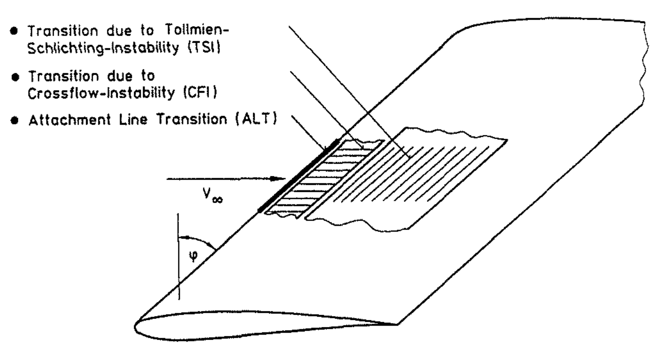

Fig. 2.1 Transition mechanisms on swept wings

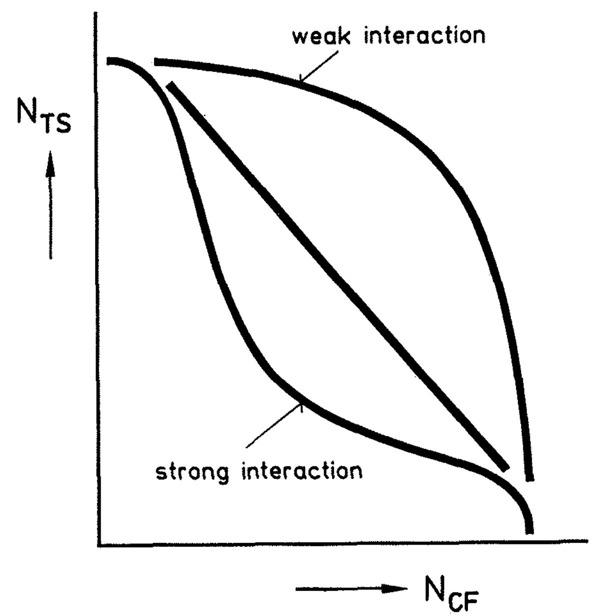

Fig. 2.3 Different types of N_{TS}-N_{CF} curves for transition prediction

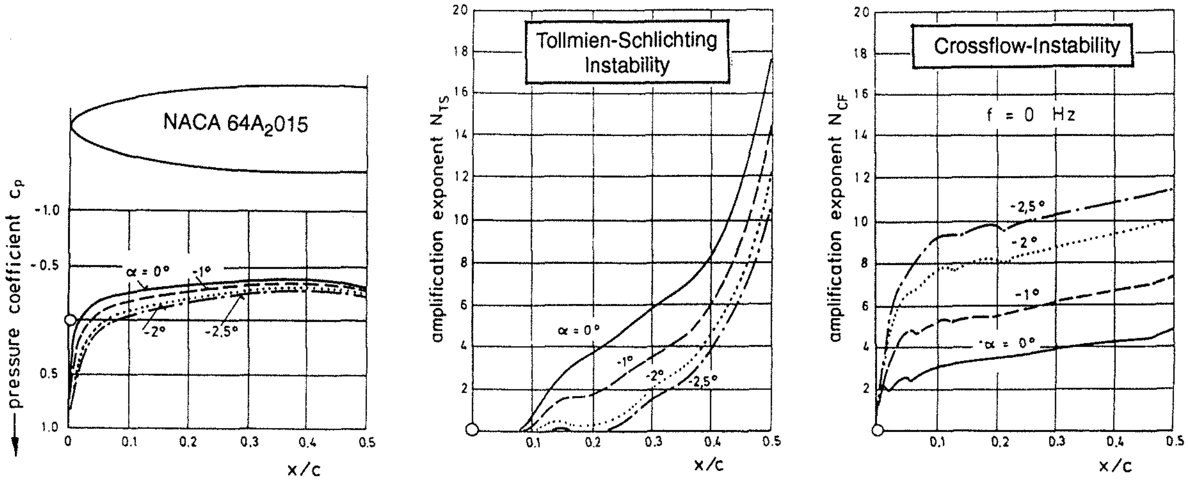

Fig. 2.2 Tollmien-Schlichting and crossflow instability on the upper surface of a NACA 64_2A015 airfoil at different angles of attack, $M = 0.27$, $Re = 15 \cdot 10^6$, $\varphi = 20^\circ$

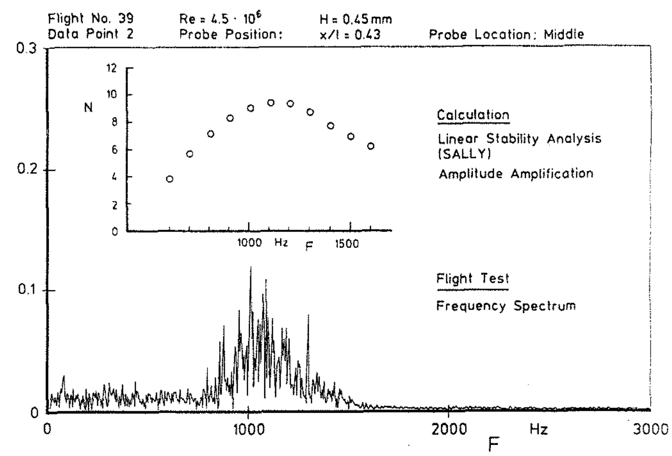

Fig. 3.2 Measured amplitude frequency spectrum in comparison with calculated N-factor spectrum

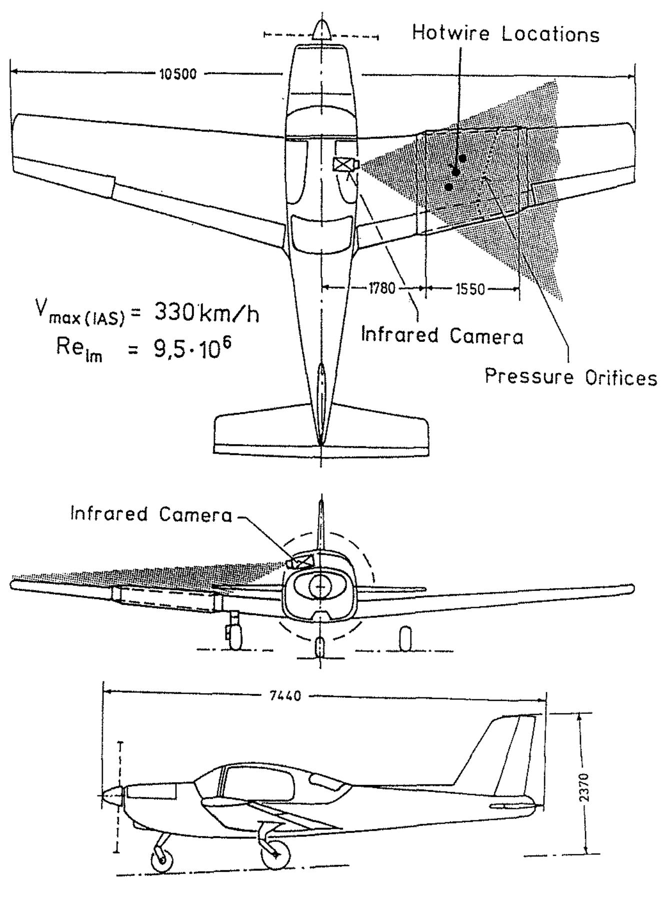

Fig. 3.1 LFU-205 aircraft with laminar glove and measurement equipment

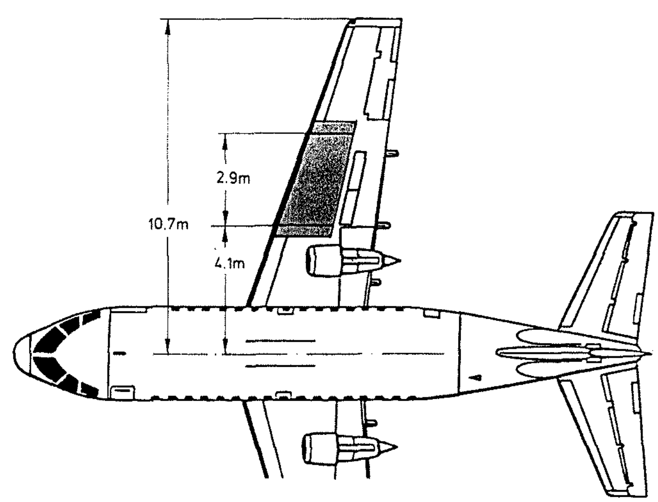

Fig. 3.3 ATTAS/VFW 614 aircraft with laminar glove

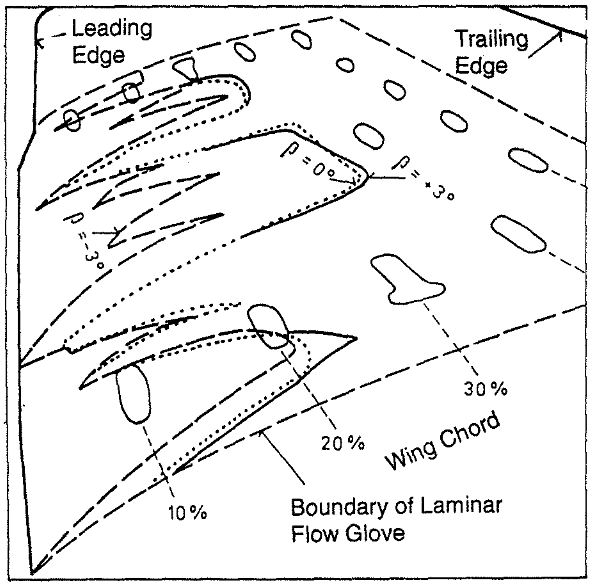

Fig. 3.4 Change of transition mechanisms by increasing yaw angles observed in flight by infrared image technique on ATTAS/VFW 614 glove ($M = 0.5$, $Re = 28 \cdot 10^6$)

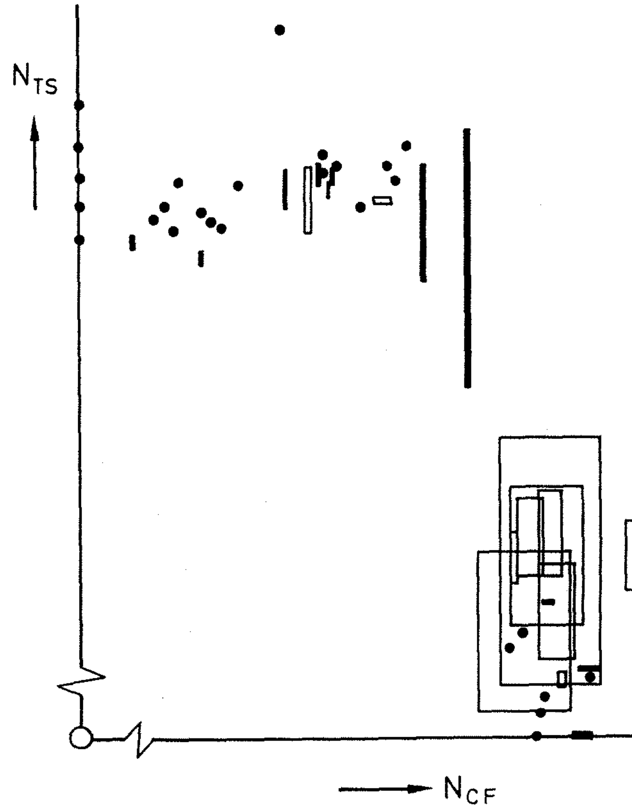

Fig. 3.5 Limiting N_{TS}- and N_{CF}-values from flight tests on the laminar flow glove of ATTAS/VFW 614

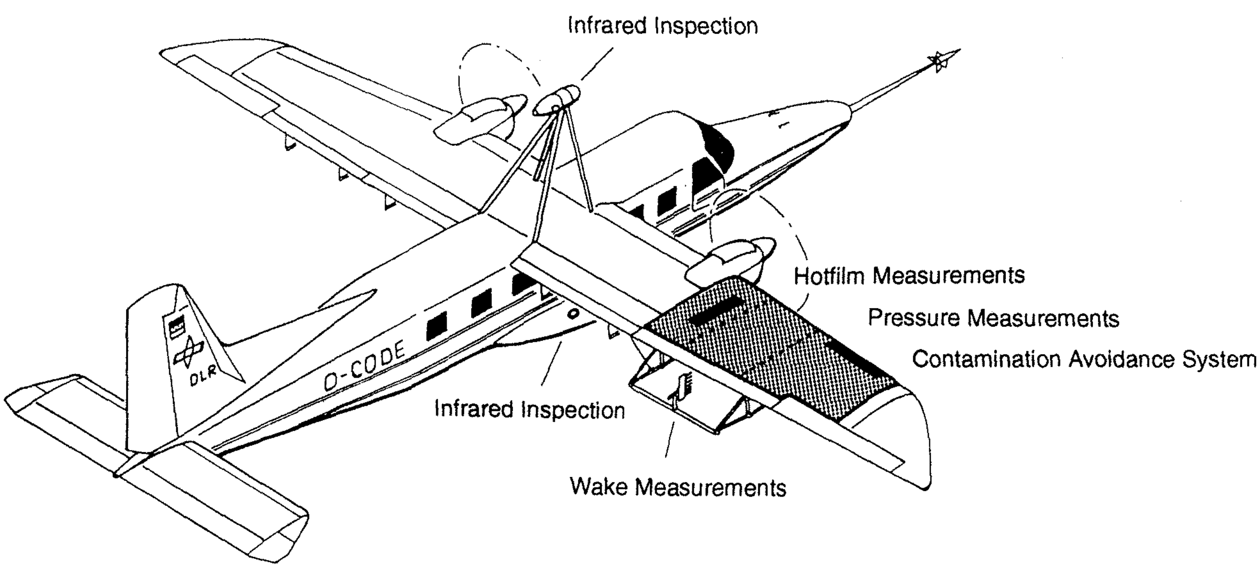

Fig. 3.6 Do 228 aircraft with laminar glove and measurement equipment

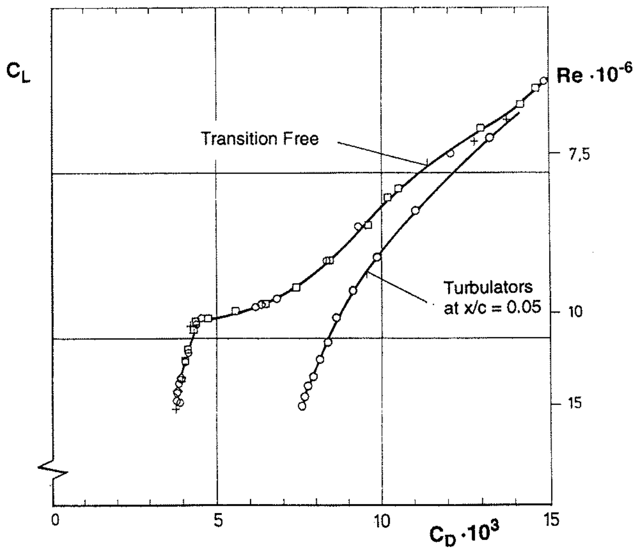

Fig. 3.7 Measured drag polars of a wing section of the laminar glove on Do 228

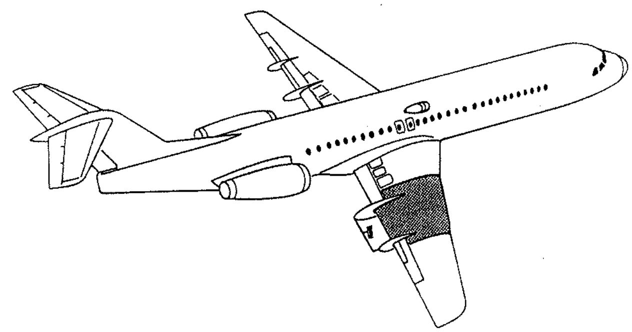

Fig. 3.8 Fokker F100 aircraft with laminar glove used in ELFIN I flight tests

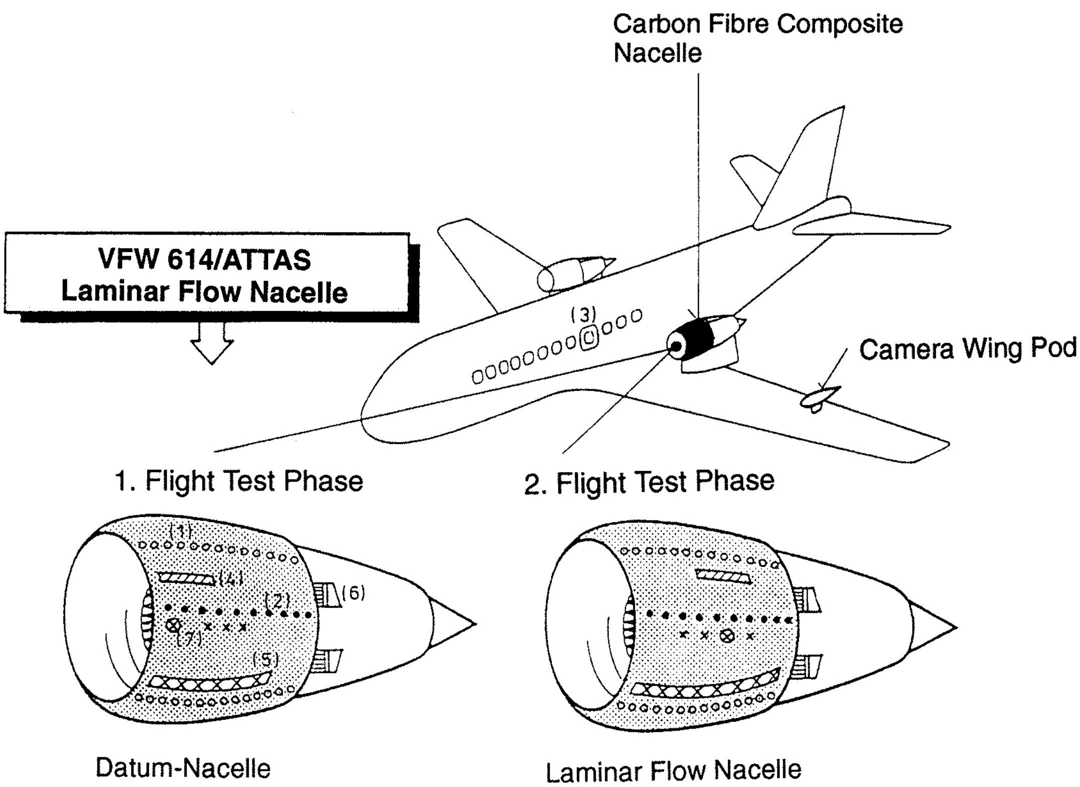

Fig. 3.9 ATTAS/VFW 614 aircraft with laminar flow nacelle and instrumentation

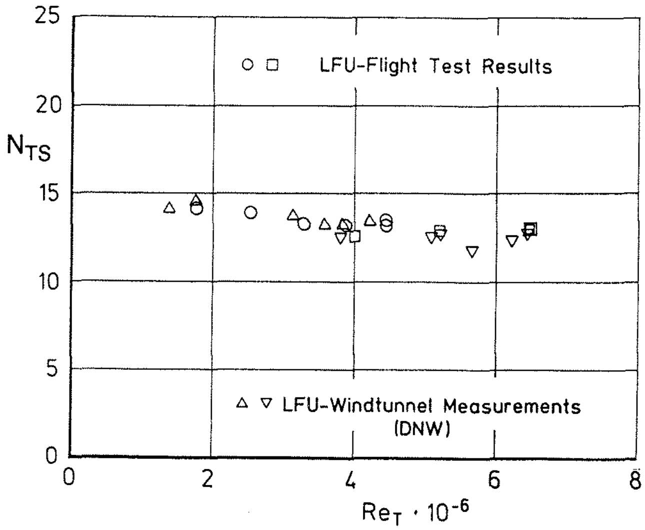

Fig. 4.1 Limiting N_{TS}-values from wind tunnel and flight tests with LFU-205

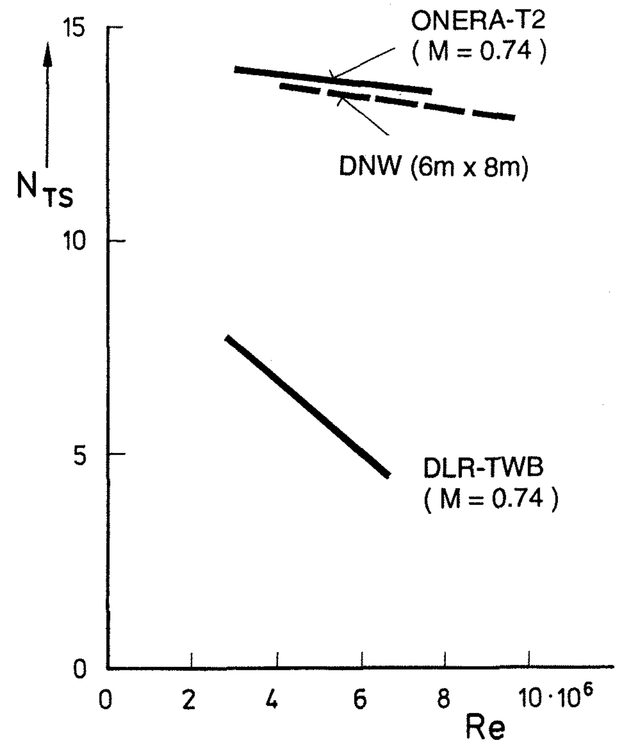

Fig. 4.2 Limiting N_{TS}-values of different wind tunnels

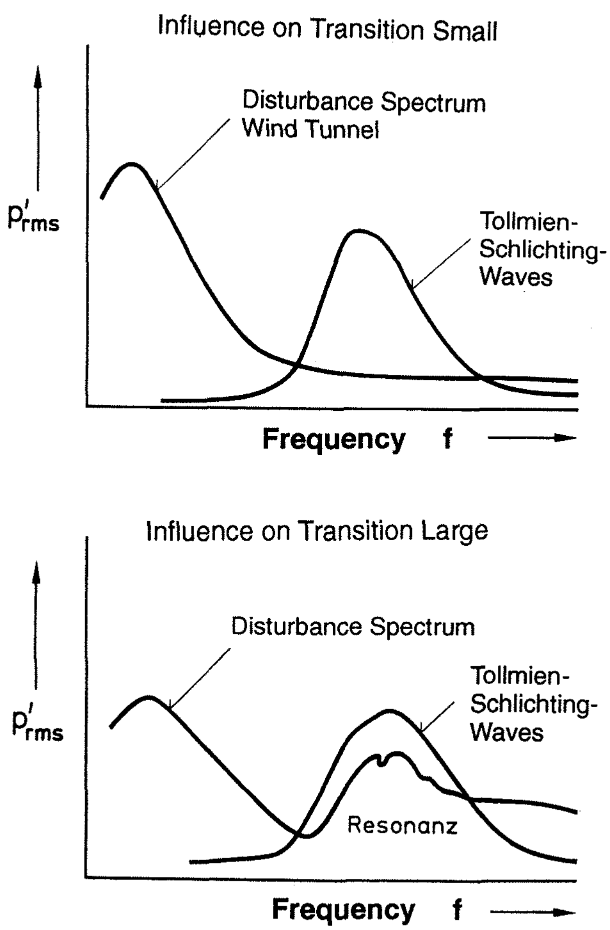

Fig. 4.4 Influence of wind tunnel disturbance spectrum on transition

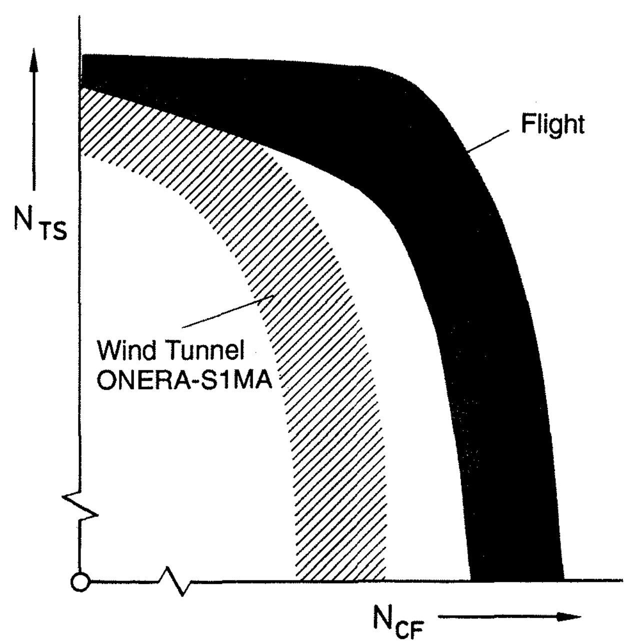

Fig. 4.3 Limiting N_{TS}- and N_{CF}-values of ONERA-S1MA wind tunnel in comparison with free flight results

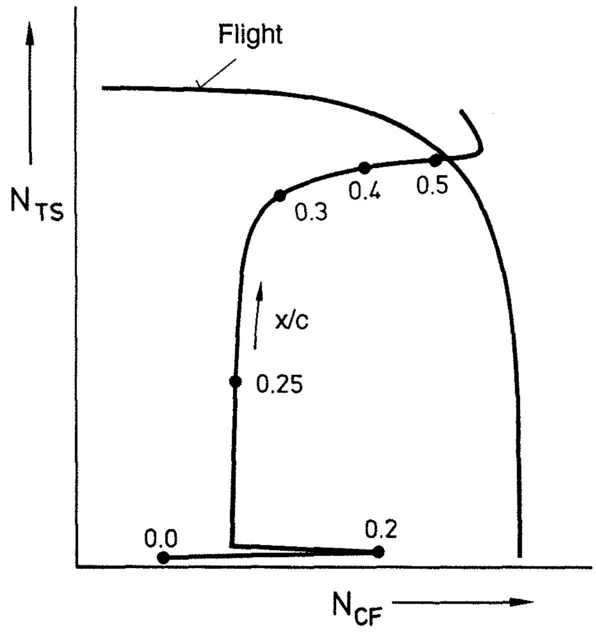

Fig. 4.5 Stability behaviour of a wing section with laminar flow in the N_{TS}-N_{CF}-diagramme at free-flight conditions (full scale)

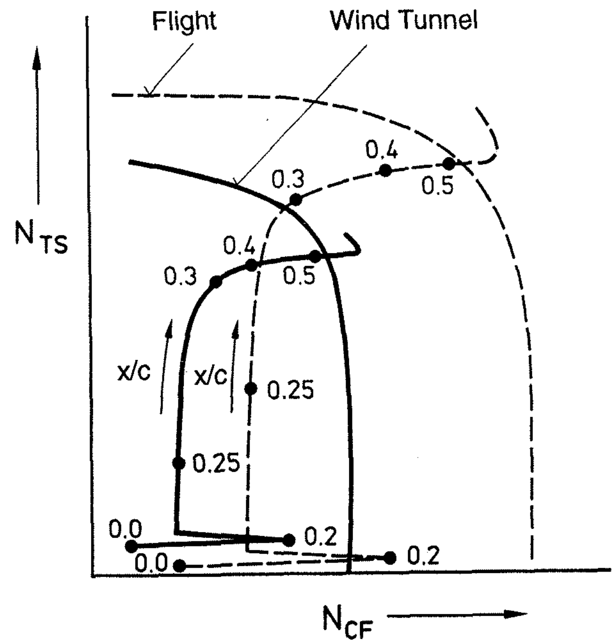

Fig. 4.6 Stability behaviour of a wing section with laminar flow in a wind tunnel with reduced flow quality and lower Reynolds number